3 Biotech (2018) 8:193
https://doi.org/10.1007/s13205-018-1221-3

ORIGINAL ARTICLE

The effect of chitosan–PMAA–NPK nanofertilizer on *Pisum sativum* plants

Noha S. Khalifa[1] · **Mohammed N. Hasaneen**[2]

Received: 24 January 2018 / Accepted: 16 March 2018 / Published online: 21 March 2018

Abstract

The use of chitosan (CS) as a carrier for slow fertilizer release is a novel trend. The potential effect of this system in agriculture is still debatable. Here, chitosan (CS) nanoparticles were obtained by polymerizing methacrylic acid (PMAA) for the entrapment of nitrogen, phosphorous and potassium (NPK) nanoparticles (NP), each at a time to form CS–PMAA–NPK NPs complex. The impact of this complex was evaluated using garden pea (*Pisum sativum* var. Master B) plants. Five-day-old pea seedlings were treated through their root system with CS–PMAA–NPK NPs at concentrations of 1, 0.5, 0.25, 0.125 and 0.0625 of the stock solution (*R*) for 1, 2, 4 and 7 days. In general, CS–PMAA–NPK NP complex reduced root elongation rate and resulted in the accumulation of starch at the root tip in a dose-dependent manner within the treated plants. Interestingly, the lowest concentrations of 0.0625 and 0.125 *R* had induced mitotic cell division (MI = 22.45 ± 2.68 and 19.72 ± 3.48, respectively) compared with the control (MI = 9.09 ± 3.28). In addition, some of major proteins such as convicilin, vicilin and legumin β were upregulated in plants treated with these low concentrations too. However, all concentrations used exhibited genotoxic effect on DNA based on the comet assay data after 48 h of treatment. Thus, it is highly recommended to consider the negative effects of this carrier system on plants and environment that may arise due to its accumulation in the agricultural fields.

Keywords Nanochitosan–NPK · Root elongation assay · Comet assay · Mitotic Index · Protein electrophoresis

Abbreviations

CS	Chitosan
DMSO	Dimethyl sulfoxide
DTT	Dithiothreitol
EDTA	Ethylenediaminetetraacetic acid
LMA	Low-melting agarose
NPK	Nitrogen phosphorous potassium
NPs	Nanoparticles
PBS	Phosphate buffer Saline
PMAA	Polymerizing methacrylic acid
PMSF	Phenylmethyl sulfonylfluoride
R	Stock solution
SDS-PAGE	Sodium dodecyl sulfate-polyacrylamide gel electrophoresis
TAE	Tris–acetic acid–EDTA

✉ Noha S. Khalifa
nohakhalifa@hotmail.com

[1] Botany Department, Faculty of Science, Ain Shams University, Cairo, Egypt

[2] Botany Department, Faculty of Science, Mansoura University, Mansoura, Egypt

Introduction

The quality of crop plant is largely dependent on the quantity of fertilizer and water. Using nitrogen, phosphorous and potassium (NPK) is mostly a key management strategy for enhancing plant productivity (White and Brown 2010). The world demand for nitrogen, phosphate and potassium was estimated to increase from 1.4 to 2.6 percent between 2014 and 2018 and is forecasted to be progressively increased (FAO 2015). Unfortunately, up to 70% of nitrogen, 90% of phosphorus and 70% of potassium are lost and drained through soil into major water banks (Alfaro et al. 2008). This will result in great value loss in agribusiness besides serious environmental pollution (Good and Beatty 2011). For instance, toxic level of nitrogen accumulation in water streams and the consequent algal bloom is one of the major problems affecting aquatic and human lives (Halling-Sorensen and Jorgensen 1993; Jiao et al. 2017).

Plant fertilizers can be applied through the soil (for uptake by plant roots), through foliar spray (for uptake through leaves) (O'Neill et al. 2014) or both ways together (Yan et al. 2018). In this connection, carrier delivery

systems of nano-fertilizers can synchronize their release with their uptake by crops thus preventing undesirable loss of nutrients to soil (DeRosa et al. 2010). The actual application of delivery system for nanofertilizers came rather recently in agriculture (Joseph and Morrison 2006; Kuzma and Verhage 2006; Roco 2011; Scott and Chen 2013). Chitosan (CS) is among polymers with high preference to be used in this respect (Janes et al. 2001; Corradini et al. 2010). Nano-CS had been used to deliver pesticides (Radhakrishnan et al. 2015), herbicides (Celis et al. 2012), plant hormones (Pereira et al. 2017), genetic material for plant transformation (Sivamani et al. 2009), macronutrients for crop growth promotion (Abdel-Aziz et al. 2016) and many others (Kashyap et al. 2015). Chitosan is characterized by its biocompatibility, biodegradability, nontoxicity, and adsorption abilities when used at the right concentration (Pang et al. 2017). Chitosan matrix acts as a protective reservoir for loaded agrofertilizers, where it allows their gradual release to the environment. At the nanosize, CS acts as an elicitor that mimics the action of a plant pathogen (Malerba et al. 2012). It can induce signaling transduction pathway that appears to target DNA at the end (Malerba and Cerana 2016). Yet, the actual biological function of CS needs further investigation (Lizardi-Mendoza et al. 2016).

CS–PMAA–NPK NPs had been reported and characterized at the physical level (Corradini et al. 2010; Hasaneen et al. 2014). Nano-chitosan–PMAA–NPK NPs, applied at relatively low concentration as foliar spray, enhanced the growth and productivity of wheat plants (Abdel-Aziz et al. 2016). However, no attempts have been done to explore the concentration-dependent behavior of CS–PMAA–NPK NPs at the molecular level in plants when it is applied via the root system.

Therefore, the objective of this study was to determine the effect of CS–PMAA–NPK NPs on some molecular aspects of *Pisum sativum* as a model plant. This evaluation was based on the effects of applying different concentrations of the nanofertilizer CS–PMAA–NPK on root elongation rate, starch accumulation at the root tips, SDS-PAGE protein profile, rate of mitosis and genotoxic effect at the DNA level based on comet assay data analysis.

Materials and methods

Plant material

Pisum sativum seeds were purchased from the Agricultural Research Center, Ministry of Agriculture, Cairo, Egypt, as "Master B" true breeding line.

Preparation and characterization of chitosan–PMAA–NPK NPs mixture

Chitosan–polymethyacrylic acid (PMAA) nanoparticle suspension with entrapment of NPK was prepared by polymerizing N, P, or K, each at a time, in CS–PMAA solution in two steps as described by Corradini et al. (2010). Briefly, 2 g chitosan were dissolved in 100 ml acetic acid (2%) and placed on magnetic stirrer at 60 °C until being fully dissolved. The 2% chitosan solution was then mixed with 0.5% PMAA (V/V) and left on magnetic stirrer at 60 °C for further 12 h. The PMAA-mediated polymerization reaction between CS–PMAA and other elements, i.e., N, P or K was achieved via oxidative decarboxylation, using potassium peroxodisulfate ($K_2S_2O_8$). All prepared solutions were lyophilized using speedvac (Thermo Savant, USA) and used in the preparation of the stock solution. Stock solution (*R*) concentration stands for 500 ppm of N, 60 ppm of P and 400 ppm of K. All other concentrations of 1, 0.5, 0.25, 0.125 and 0.0625 *R* were made from the serial dilution of this stock solution. Surface morphology and sizes of all nanoparticles were examined by JOEL 1010 transmission electron microscope. This was done to assure that the produced particles were homologous in size and morphology. All solutions were prepared in the nanobiotechnology lab (Faculty of Science, El Mansora University, Egypt) following the protocol of Hasaneen et al. (2014). The mixture was stable and could maintain its molecular distribution for up to 2 years in fridge.

Zeta potential measurement

Zeta potential is used to determine the optimum pH value at which any solute distributes homogenously within the solvent; i.e., without agglomeration. Zeta potentials of CS–PMAA, CS–PMAA–N, CS–PMAA–P and CS–PMAA–K were measured at different pH values using nano zetasizer device (NZS, Malvern Ltd., Worcestershire, England).

Experiment layout

Seeds with homogenous color and size were soaked in distilled water overnight and then washed three times with 15% bleach followed by washing in sterile distilled water. Seed planting was carried out on wet filter paper in the growth chamber at 20 °C in dark. After germination, the growth chamber was adjusted at 8/16 h light/dark cycles at 20 °C. Roots of 1 cm in length (~ 5-day-old seedlings) were soaked in different concentrations of CS–PMAA–NPK nanoparticles for 1, 2, 4, 7 days on freshly prepared Petri plates. The stock solution (1 *R*) was serially diluted into 0.5, 0.25,

0.125 and 0.0625 *R*. Different applications at the selected time course were followed afterwards. To determine root elongation rate, seedlings were arranged side by side on a black background and photographed using digital camera (Sony Cyber-Shot, 12.1 MP, DSC-W200, Japan) 2, 4 and 7 days after treatment. Total root length of scaled images was measured using the ImageJ software program (https://imagej.nih.gov/ij/download.html). Root length means (*M*), standard deviation (SD), *p* values for significance, and *T* test were calculated using excel software program.

Starch content in roots

Intact roots of the plants treated with different concentrations of CS–PMAA–NPK NPs (for 48 h) were stained with iodine–potassium iodide (I_2–KI) solution (0.15% [w/v] I_2 and 0.45% [w/v] KI) for 15 min and analyzed as mentioned by Sedbrook et al. (1999). Root pictures were taken using the stereomicroscope (Leica microsystem, Wetzlar, Germany).

Mitotic Index and cell division rate

The method of Niki and Gladish (2001) was followed with some modifications. Briefly, root tips were excised right after the treatment time, fixed in Carnoy's solution (ethanol:glacial acetic acid in 3:1 ratio) and incubated for 24 h at 4 °C. Roots were stored in 70% ethanol at 4 °C until ready to use. Root tips were hydrolyzed in one normal hydrochloric acid (1 N HCl) for 12 min at 60 °C and then stained with 2% aceto lacto-orcin in acetic acid for 30 min, and finally squashed on a slide with a drop of 45% acetic acid in water. Squashed tissues were manually examined for different phases of mitosis (interphase, prophase, metaphase, ana-telophase) under the light microscope on the same day of slide preparation. Data were statistically analyzed using excel program. Micrographs were captured using Leica (DM 2500, Wetzlar, Germany) and analyzed using Image Processing Analysis software (Leica CW4000, Wetzlar, Germany).

Total soluble protein extraction and SDS-PAGE electrophoresis

Proteins were extracted from 5-day-old seedlings after being soaked in the applied concentrations of 1, 0.5. 0.25, 0.125 and 0.0625 *R* of CS–PMAA–NPK NPs for 48 h as described by Khalifa (2012). Briefly, whole seedlings were ground in liquid nitrogen and then homogenized in Tris–HCl buffer (Sigma-Aldrich, St. Louis, MO, USA) at pH 8 (W/V); 0.1 mM phenylmethyl sulfonylfluoride (PMSF) as protease inhibitor and 100 mM dithiothreitol (DTT) as a reducing agent (instead of mercaptoethanol). All steps were carried out on ice. Total soluble proteins were collected by centrifugation at 4 °C and 15,000 rpm for 15 min. Protein concentrations in different samples were measured spectrophotometrically using Pierce Coomassie protein assay kit (ThermoScience, USA) in relation to BSA standard. Equal amounts of protein extracts were loaded onto the gel (~ 20 µg/lane) and run onto 12% polyacrylamide gel in the presence of sodium dodecyl sulfate-polyacrylamide Gel electrophoresis (i.e., SDS-PAGE). Preparation and staining of the gel were carried out as described by Laemmli (1970). Electrophoresis was performed at 100 V using Omni-PAGE Mini Wide vertical unit (Cleaver Scientific, UK). Major protein bands of pea plants separated by SDS-PAGE electrophoresis were identified according to Barac et al. (2010).The experiment was repeated three times for confirming its reproducibility.

Comet assay

Isolation of intact nuclei

Nuclei were isolated from the root tip cells after treatment with different concentrations of 1, 0.5. 0.25, 0.125 and 0.0625 *R* of CS–PMAA–NPK NPs for 24 and 48 h following the method of Nikolova et al. (2013) with some modifications. Briefly, 3–4 root tips were cut into fine pieces on ice with pre-frozen fresh razor blade in 300 µl homogenization buffer (0.4 M Tris-HCl, pH 7.5) (Gichner et al. 2006). The white lysate with nuclei was collected without large clumps of tissues and kept on ice during the time course of the experiment. It is noteworthy to mention that filtration through a 50-µm nylon filter, as described in Rodriguez et al. (2011), was unnecessary.

Slide preparation

Normal melting point (NMP) agarose (0.5 ml of 1% (w/v) in water) was added while warm on slide then leveled with a cover slip to form a uniform gel layer. The slide was kept at room temperature for 15 min, then the cover slip was removed using a cutter tip and kept in the fridge until used (~ 1–2 h). The nuclear suspension, 100 µl of cell lysate, was gently mixed with 100 µl of 1% LMP (Low Melting Point) agarose in phosphate buffer saline (PBS buffer) at 40 °C by repeated pipetting, using a cut pipette tip, then added onto the slide and leveled with a cover slip. The slides were kept in the fridge for 15 min to 1 h, and then the cover slip was carefully removed to avoid the formation of either air bubbles or distorting the underneath gel layer. According to the results obtained, it was unnecessary to add a third layer of LMA agarose as mentioned by Nandhakumar et al. (2011).

Cell lysis

Cell lysate pre-coated slides were placed in cold lysis buffer (2.5 M NaCl, 10 mM ethylenediaminetetraacetic acid (EDTA), pH 8, 10 mM Tris–HCl, pH 8, 1% N-lauroylsarcosine sodium salt, 1% Triton X-100 and 10% dimethyl sulfoxide (DMSO)) and incubated in dark for 90 min at 4 °C according to Nandhakumar et al. (2011). DMSO was added right before the incubation time; otherwise it would cause the lysis solution to form white crystals.

Neutral comet assay

Slides were prepared according to Nandhakumar et al. (2011) with some modifications. Slides were neutralized in cold 1× Tris–acetic acid–EDTA (TAE), pH 8 for 20 min in the fridge then arranged in a horizontal gel electrophoresis tank containing cold 1× TAE, pH 8. Slides were subjected to electrophoresis at ~20 V for 40 min at 4 °C. After electrophoresis, slides were dehydrated in 70 and 95% for 5 min each and prepared for staining.

Giemsa staining

The protocol of Osipov et al. (2014) was followed with some modifications. Briefly, slides were immersed in 5% Giemsa stain working solution (Merck, Darmstadt, Germany) in distilled water for 30 min and then washed in PBS buffer (pH 7.5) until the washout became clear from the blue color of the stain. Three slides per treatment were prepared from four plants and examined under the bright-field light microscope (Optica microscope, Italy).

Data analysis

Digital images were scale calibrated and the diameter of intact nucleus or the total length of comet structure was measured using ImageJ program software (Schneider et al. 2012). Differences between treated and untreated groups were statistically evaluated using the paired *T*-test.

Results

Characterization of the CS–PMAA–NPK NPs complex

The sizes of nanoparticles used in this study were determined from their corresponding TEM micrographs. The average diameter length of CS–PMAA was 19.68 nm ± 5.51 (Fig. 1a). CS–PMAA loaded with nitrogen, phosphorous or potassium, each at a time, exhibited diameters of

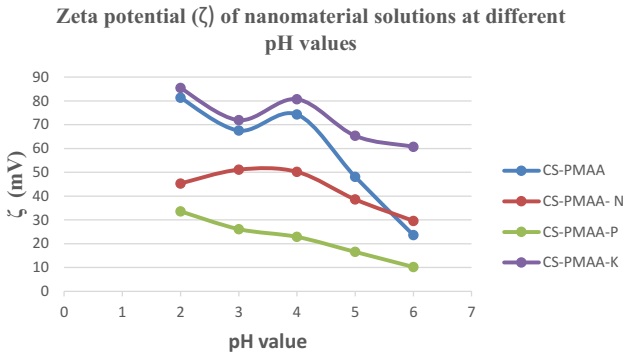

Fig. 2 Graphical representation of zeta potential of the nanomaterial used at different pH values. The concentration used for each nanomaterial was the same as that used for plant treatment

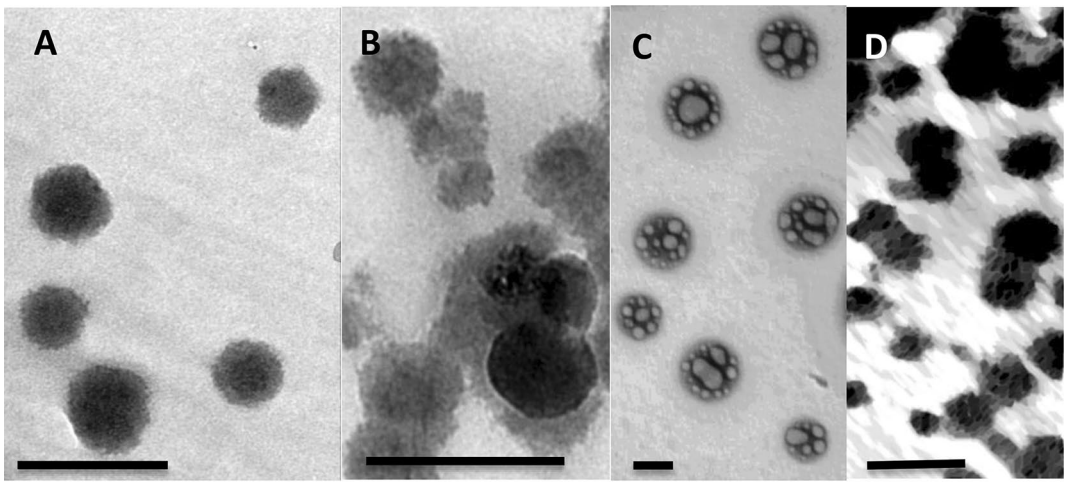

Fig. 1 Representative TEM images of nanoparticles used in this study. Images are showing **a** Chitosan–PMAA alone or with **b** nitrogen; **c** phosphorous and **d** potassium. Scale bar = 50 nm

38.98 nm ± 5.29, 87.65 nm ± 11.85 and 24.07 nm ± 4.19, respectively (Fig. 1b–d). The dispersion of nanoparticles was homogenous without any agglomeration (Fig. 1a–d). The stability of each mixture at different pH values was checked by calculating zeta potential value (Fig. 2). The highest zeta potential for all solutions used was detected at pH range ~4.5–5.

Root elongation bioassay

A significant reduction in root length was shown after treatment with CS–NPK–NP mixture in a dose-dependent manner, compared to the control (Fig. 3a, b, Table 1). At higher concentrations (1 and 0.5 *R*), lateral root formation was completely inhibited either when plants were grown vertically in test tubes (Fig. 3a) or when seeds were immersed in Petri dishes (Fig. 3b). At this stage, no abnormalities were observed within the shoot system of seedlings.

Fig. 3 **a** Effect of different concentrations of CS–NPK NPs on root growth and lateral root formation. Representative picture of pea seedlings grown for 7 days in the presence of different concentrations of CS–NPK nanoparticles. Seedlings were grown either **a** vertically in test tubes or **b** immersed horizontally in Petri dishes supplemented with the applied concentrations. Note the inhibition of lateral root formation at higher concentrations of 1 and 0.5 *R*

Starch accumulation

The highest concentration (*R*) of CS–PMAA–NPK NP resulted in the accumulation of starch at the root tip after 7 days treatment (Fig. 3c). The death rate was high among the seedlings treated with 1 and 0.5 *R*. Death percentage was up to 70% after 2 days in treatments with 1 and 0.5 *R*. On the other hand, starch accumulation level was not distinguishable from the corresponding control in the plants treated with the lowest concentration of the nanofertilizer (0.0625 *R*) (Fig. 4c).

Mitotic Index and cell division rate

The rate of cell division represented by the Mitotic Index value was higher in the plants treated with 0.0625 *R* (22.45 ± 2.68) and 0.125 *R* (19.72 ± 3.48), compared with that of control (9.09 ± 3.28). The reduction in Mitotic Index was proportional with the dose applied at concentrations higher than 0.125 *R* as shown in Table 2. Major abnormalities observed in cells during interphase included nuclei that were fragmented, apoptotic, vacuolated or constricted with many nucleoli (Fig. 5). At metaphase, sticky and dispersed chromosomes were also detected (Fig. 5). The highest concentrations (*R* and 0.5 *R*) resulted in complete mitotic arrest.

Total soluble protein

Convicilin, vicilin 1, 2 and 3, and legumin β exhibited higher expression, than that of the control, as a result of treatments with 0.0625 and 0.125 *R* (Fig. 6). Legumin α was upregulated only in the plants treated with 0.0625 *R* (Fig. 6). The expression of all the previously mentioned proteins was

Table 1 Results of the root elongation assay of *Pisum sativum* seedlings treated with different concentrations of chitosan–NPK nanofertilizer

Treatment time (days)	Concentration					
	Control (0)	0.0625 *R*	0.25 *R*	0.125 *R*	0.5 *R*	*R*
2 days (M ± SD)	3.42 ± 0.64	1.11 ± 0.19 $P = 2.7 \times 10^{-5}$	1.60 ± 0.4 $P = 0.0016$	1.5 ± 0.2 $P = 0.005$	1.18 ± 0.12 $P = 0.0001$	0.97 ± 0.42 $P = 7.7 \times 10^{-5}$
4 days (M ± SD)	3.97 ± 0.82	3.97 ± 0.63 $P = 0.008$	2.87 ± 0.63 $P = 0.019$	2.33 ± 0.13 $P = 0.02$	2.26 ± 0.17 $P = 0.003$	1.85 ± 0.15 $P = 0.011$
7 days (M ± SD)	5.38 ± 0.44	4.55 ± 1.62 $P = 0.116$	4.19 ± 0.98 $P = 0.044$	3.85 ± 0.68 $P = 0.0006$	3.68 ± 0.68 $P = 0.00074$	2.21 ± 0.01 $P = 0.0024$

The root lengths were measured in cm using ImageJ program software. *R* = stock solution concentration (1 mg l^{-1})

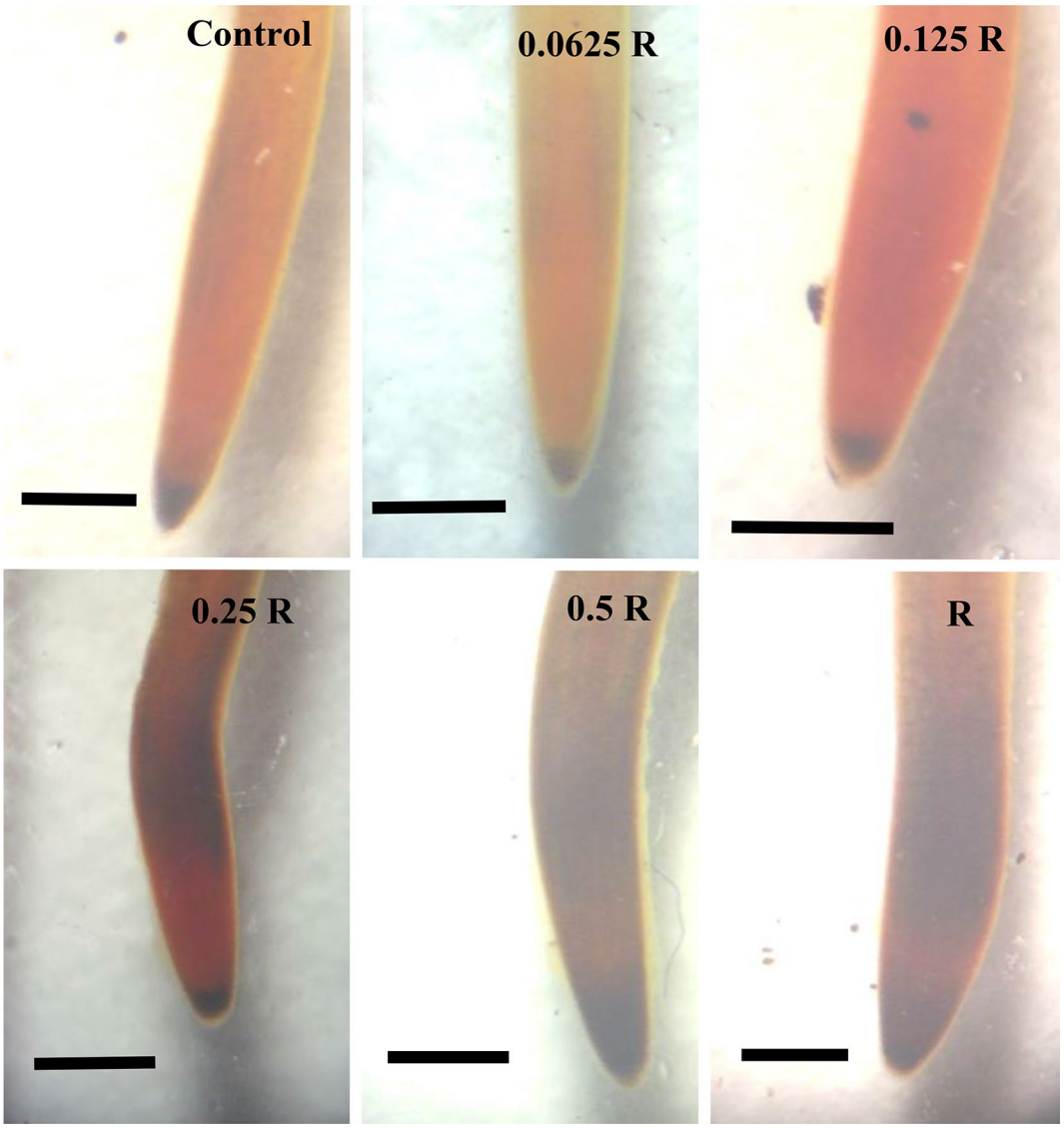

Fig. 4 Starch accumulation after 48 h treatment. Starch accumulation at root tip increased at higher concentrations. It was also observed that starch was accumulated in the root hair zone in plants treated with 0.25, 0.5 and 1 *R* in a dose-dependent manner. Scale bar = 5 mm

Table 2 Cell division rate as measured by Mitotic Index (MI) in the plants treated with different concentrations of CS–NPK–NP for 48 h

	Concentration					
	Control (0)	0.0625 *R*	0.125 *R*	0.25 *R*	0.5 *R*	*R*
MI ± SD	9.09 ± 3.28	22.45 ± 2.68	19.72 ± 3.48	7.11 ± 3.92	5.32 ± 4.33	4.67 ± 4.20

R = stock solution concentration (1 mg l^{-1})

reduced in a dose-dependent manner at 0.25 *R* or higher concentrations (Fig. 6).

Comet assay analysis

High death rate was observed due to treatments with *R* and 0.5 *R* CS–PMAA–NPK NPs. Unfortunately, intact nuclei could not be obtained in treatment with these relatively high concentrations (*R* and 0.5 *R* CS-PMAA-NPK NPs) to carry out the comet assay, since the isolated nuclei were highly fragmented. Thus, comet assay for *R* and 0.5 *R* treatments was excluded. The DNA damage induced by the CS–PMAA–NPK NPs was directly proportional

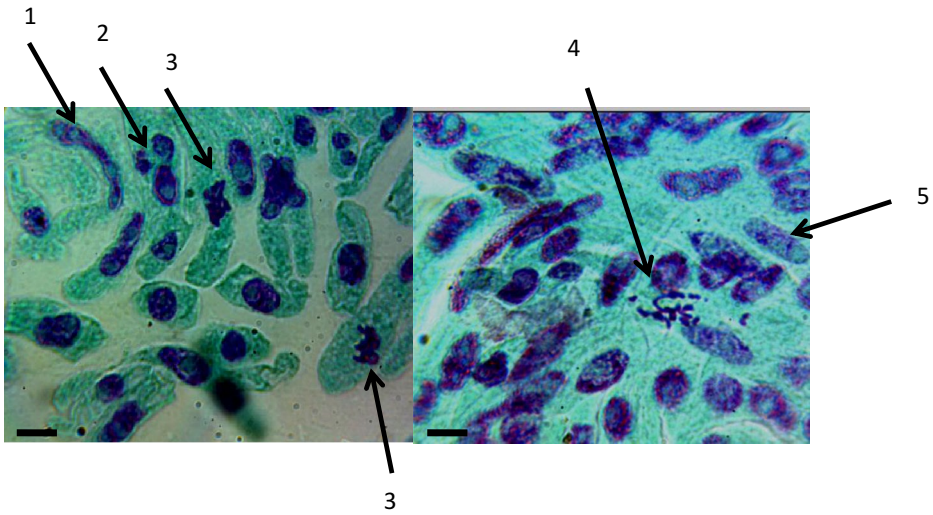

Fig. 5 Cytological analysis of plants treated with high concentration (1 and 0.5 *R*) of chitosan–NPK nanofertilizer. Elongated nucleus with three nucleoli (1); micronucleus that resulted likely from chromosomal breaks (2); sticky metaphase (3); dispersed metaphase (4) and vacuolated nucleus (5). Scale bar = 1 µm

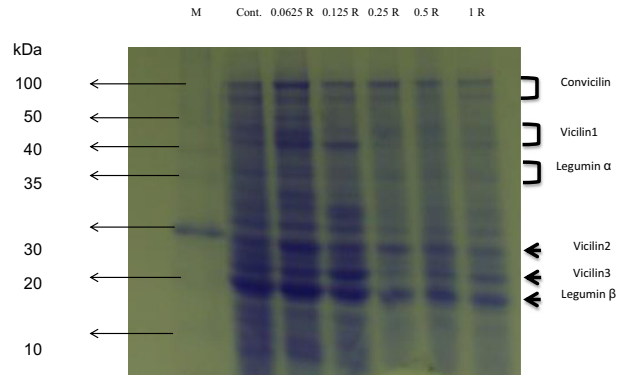

Fig. 6 SDS-PAGE electrophoretic patterns of total soluble pea proteins treated with different concentrations of CS–NPK–NP for 48 h. Note the change in protein profile in response to different treatments compared to the control

to the applied dose and the duration time of treatment (Fig. 7). Control plants contained normal undamaged cells with intact nuclei (Fig. 7a). Following treatment with CS–PMAA–NPK NPs for 24 h, the relatively low concentrations of CS–PMAA–NPK NPs (0.0625 and 0.125 *R*) exhibited slight DNA stretching toward the anode (+) with nuclei diameters of 23.63 ± 10.12 and 26.51 ± 4.66 µm, respectively. This slight DNA migration caused by either of these two concentrations was not significant with p values of $p = 0.18$ and 0.90, respectively, compared with that of the control where the diameter of the nucleus was 22.04 ± 5.89 (Table 3). On the other hand, in case of treatment with CS–PMAA–NPK NPs at the concentration 0.25 *R* for 24 h or all concentrations for 48 h, the cells exhibited DNA tails that were significantly longer than those of corresponding controls (Table 3).

Discussion

Nanofertilizers had been used before in agriculture (Morales-Díaz et al. 2017) and showed great ability to enhance the growth of many crop plants such as rice (Wang et al. 2011), okra (Mondal et al. 2012) and Chinese cabbage (Baskar et al. 2015). Several studies, on the other hand, documented toxic effects of nanoparticles in higher plants (Dimkpa et al. 2013; Rajkishore 2013) and negative impact on the environment (Ray et al. 2009). Nano-chitosan enhanced the growth of corn used in combination with Rhizobacteria (Khati et al. 2017). Application of CS–PMAA–NPK NPs resulted in positive effects on the growth and productivity of wheat plants (Abdel-Aziz et al. 2016). It seems that CS–PMAA–NPK NPs enhanced wheat growth upon foliar applications in well-drained sandy soil (Abdel-Aziz et al. 2016).To date no attempts had been done to explore the potential effect of CS–PMAA–NPK NPs neither if applied directly to plant roots, nor with long-term persistence. Thus, the objective of this study was to determine the effect of CS–PMAA–NPK NP supplemented via the roots of pea seedlings at early developmental stages for increasing time intervals (1, 2, 4, 7 days). This will give an insight about the actual effect of this nanofertilizer delivery system if accumulated in soil and how it will affect newly growing plants in the field.

The results obtained indicated that the used concentrations of CS–PMAA–NPK NPs (1, 0.5, 0.25, 0.125 and 0.0625 of the stock solution *R*) reduced root elongation rate of the treated plants in a dose-dependent manner (Table 1). The relatively high concentrations (*R* and 0.5*R*) inhibited lateral root formation as well (Fig. 3a, b and Table 1) and highly reduced root elongation over the extended treatment of 7 days (Fig. 3a, b). A similar conclusion was obtained with *Brassica napus* seedlings on application of copper oxide nanoparticles at high concentrations, which resulted in

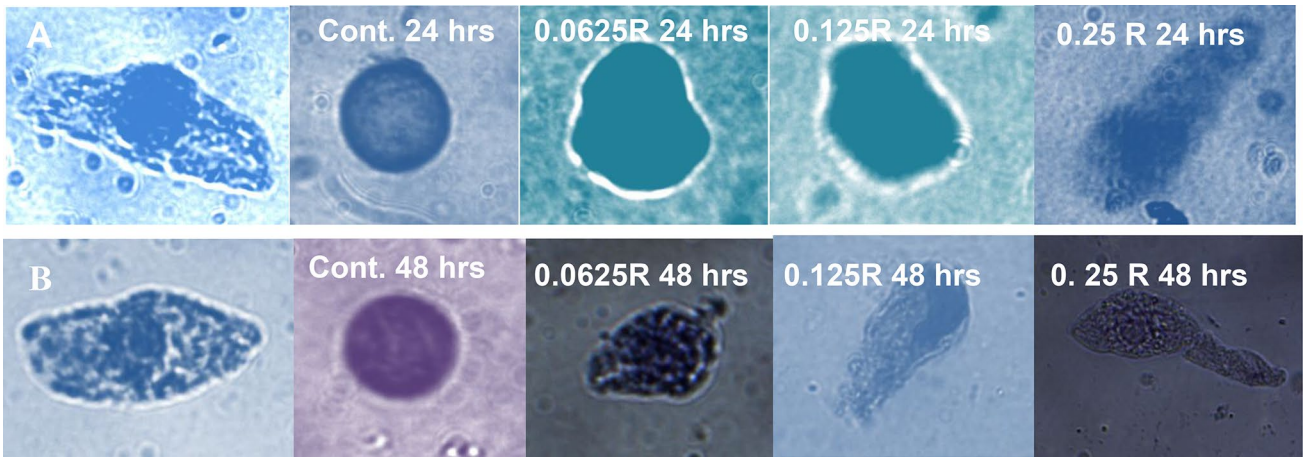

Fig. 7 DNA damage as expressed by comet assay in pea plants treated with different concentrations of CS–PMAA–NPK NPs for 24 h (upper row) and 48 h (lower row). Nucleus in intact cell before lysis in A and B to compare the nucleus size and shape. The shape of nuclei after lysis and electrophoresis in control were round and intact. The comet length was increasing with the applied concentration and the incubation time. Higher concentrations of 1 and 0.5 *R* resulted in the formation of fragmented nuclei in intact cells and, thus, were excluded from the analysis

Table 3 Genotoxic effect resulted from treating plants with different concentrations of CS–NPK–NP for 24 and 48 h

Treatment time (h)	Concentration			
	Control (0)	0.0625 *R*	0.125 *R*	0.25 *R*
24	22.04 ± 5.89	23.63 ± 10.12	26.51 ± 4.66	49.26 ± 9.97
		$P = 0.18$	$P = 0.90$	$P = 5.44 \times 10^{-6}$
48	22.29 ± 5.28	24.53 ± 3.05	34.75 ± 9.01	61.13 ± 8.19
		$P = 0.00027$	$P = 0.0069$	$P = 1.28 \times 10^{-7}$

DNA damage is corresponding to the length of comet structure, expressed as mean nucleoli diameter (μm) ± SD values. These values were directly proportional with dose concentration and incubation time. *R* = stock solution concentration (1 mg l^{-1}). *P* represents the value of significance between the treated group and control based on statistical analysis of *T*-test

a significant reduction in root length and inhibition of lateral root formation (Nair and Chung 2017). On the other hand, Barrenaa et al. (2009) observed zero to no toxicity when Au, Ag, and Fe_3O_4 nanoparticles were applied at very low concentrations on lettuce and cucumber plants. It is noteworthy to mention that we observed high death rate (60%) among the seedlings treated with 1 and 0.5 *R* of CS–PMAA–NPK NPs since the second day of treatment, whereas complete death of all seedlings treated with these high concentrations was attained at the seventh day of treatment. The mechanism by which plant growth is inhibited by high concentrations nanoparticles is still unknown (Siddiqi and Husen 2016).

An explanation might be attributed to chitosan properties such as film formation and coating (Badawy and Rabea 2011, Beenken et al. 2014), Gelling properties that may create protein–chitosan conjugates (Kumar et al. 1999; da Silva et al. 2014) and ion-chelating potential (Vold et al. 2003; Gritsch et al. 2018; Yazdani et al. 2018). Although these properties are beneficial for chitosan applications, e.g., as a biosorbent for phosphate removal from aqueous solutions, for new antibiotic-free antimicrobial technologies, herbicide and pesticide delivery, etc., but within the plant systems a different scenario may take place, so that nanofertilizer application may represent a double-edged sword. This could result in reduced water uptake, gas exchange and then retard the overall development of plant (Pereira et al. 2017). In addition, the small-sized nanoparticles could accumulate inside the plant and result in blockage of water diffusion at the cell membrane (Zhang 2003).

Higher starch content at the root tip and lateral root-forming zone was detected in treated plants. Higher content of starch was accumulated in these two zones in a dose-dependent manner (Fig. 3c). It is widely known that accumulation of storage compounds is associated with growth inhibition

(Zawaski et al. 2012; Li et al. 2016). Zawaski et al. (2012) also stated that reduction in root length and lateral root formation was directly proportional to starch accumulation.

To determine if the reduction of root length was directly connected to cell division rate, the Mitotic Index (MI) was investigated within root tip cells, 2 days after treatment. The MI values were higher in treatments with 0.0625 and 0.125 *R* (22.45 ± 3.66 and 19.42 ± 4.13, respectively) than the control (MI = 9.09 ± 0.67) (Table 2). Surprisingly, despite their high MI, roots were shorter in the seedlings of these treatments (0.0625 and 0.125 *R*). This might indicate that cell division rate is not the only factor responsible for the reduction of root elongation rate. Plants treated with higher concentrations exhibited relatively low MI values, compared with the control (Table 2). Thus, inhibition of cell division by CS–PMAA–NPK NPs might partially explain the retarded root growth in case of application of the relatively high concentration. Our result was in agreement with that of Nagaonkar et al. (2015) who stated that nanoparticles enhanced mitosis at low concentration and caused suppression at higher concentrations.

In our work, occurrence of apoptotic, vacuolated nuclei, bi and tri-nucleated cells was also recorded in response to application of the highest concentrations of *R* and 0.5 *R* (Fig. 5). Similar abnormalities were reported in *Allium* root cells upon treatment with high concentration of silver nanoparticles (Kumari et al. 2009).

Nanoparticles can interact with a variety of different cellular components including proteins and DNA. In general, treatments with nanoparticles caused altered protein expression (Hossain et al. 2015). Upregulated proteins are usually those related to antioxidant and stress tolerance, whereas down-regulated proteins are those usually responsible for cell proliferation and division (Zivic et al. 2018). Nanoparticle binding to protein, either in their native or denatured form, depends on the protein surface charge, hydrophobicity, intrinsic stability, and nanoparticle's physical characteristics (Cabaleiro-Lago et al. 2010). Various studies have concluded that nanoparticles can inhibit protein formation either by inducing its aggregation or by disrupting its assembly during the folding process (Zaman et al. 2014), particularly when applied at high concentration (Cabaleiro-Lago et al. 2010). One of the proposed mechanisms is that nano-CS can interact with histone protein and consequently affect the differential expression of many cellular proteins (Klosterman et al. 2003; Zhang 2003). Moreover, the gelling properties of chitosan could create protein–chitosan conjugates (Kumar et al. 1999; da Silva et al. 2014). To determine if this is the case, we performed SDS-PAGE protein electrophoresis for 2-day treated plants (Fig. 6). SDS-PAGE protein electrophoresis is a well-established technique to measure differential gene expression after treatment with substances such as nanoparticles (Cedervall et al. 2007). In this work, major protein bands in pea plants were identified according to Barac et al. (2010). As depicted in Fig. 6, no new protein bands were detected. Interestingly, the expression of some proteins such as convicilin, vicilin 1, 2 and 3, and legumin α and β were upregulated in the plants treated with the lowest concentration of CS–PMAA–NPK NPs (0.0625 *R*). The results also indicated that major bands of some proteins were markedly down-regulated in a dose-dependent manner at the concentrations higher than 0.0625 *R*, compared to the control. For instance, the expression of convicilin, legumin β and vicilin proteins were progressively reduced as the concentration of the applied nanofertilizer increased (Fig. 6). However, alteration of gene expression by chitosan might be well expected according to other workers that revealed eliciting action in some plants, induction of defense responses to abiotic and biotic stresses in plants (Malerba and Cerana 2016), increases in cytosolic Ca^{2+} (Zuppini et al. 2003), activation of MAP-kinases (Yin et al. 2010), chromatin alterations (Hadwiger 2013), synthesis of phytoregulators as jasmonate and ABA (Iriti and Faoro 2008).

To determine if CS–PMAA–NPK NPs can induce DNA damage, single-cell gel electrophoresis assay (comet assay) was used. The first comet assay using plants was published during late nineties (Koppen and Cerda 1997). Later on, the technique was extensively used to measure genotoxicity after treatment with heavy metals (Gichner et al. 2008), irradiation (Wang et al. 2013) and nanomaterials (Di Bucchianico et al. 2017). In our work, nuclei isolated from the untreated plants were intact with a diameter of ~ 22 µm during the whole course of treatment (Fig. 7). Unfortunately, we could not isolate intact nuclei from plants treated with higher concentrations of 1 and 0.5 *R*. It seemed that these high concentrations caused major nuclei damage; therefore, these two treatments were excluded from comet analysis. Comet length was proportional to the increase of nanofertilizer concentration and the incubation time in all other treatments (Fig. 7). Although overestimation of DNA-induced damage has been suggested before for comet assay analysis, using nuclei isolated from human epithelial cells incubated with NPs (Ferraro et al. 2016), our results indicated the efficiency of this technique to measure DNA genotoxicity. This is because: (a) the results of comet assay were concomitant with the nanofertilizer-triggered effects in a dose-dependent manner, and (b) the corresponding reduction in root length, mitosis and the accumulation of starch particularly at higher concentrations were obviously in alliance with the magnitude of the comet DNA genotoxicity.

However, since chitosan compounds have been demonstrated to induce numerous biological responses in plants, dependent on its concentration as well as the plant species and its developmental stage (Malerba and Cerana, 2016), we highly recommend to conduct further study to identify the appropriate safety doses and outweigh the potential toxicity

of this putative nanofertilizer with different crops, soils and ecological conditions, and to define the appropriate time and method of application. This will precisely evaluate its impact on society, environment and health before using it in the open field.

Conclusion

All data clearly indicated that the used nanoparticle caused tangible toxicity in the treated plants at high concentrations. However, the accumulative effect of low concentrations should not be neglected particularly if this nanofertilizer is applied to edible crop plants or those near to main water streams. Thus, it is highly recommended to adopt an efficient containment plan when using such nanofertilizer system even at low concentrations to assure biosafety. This microscale experiment reflects indeed what will happen if this carrier system is applied directly to the agricultural soil and accumulates in the field after several applications.

Funding This research did not receive any specific grant from funding agencies in the public, commercial, or non-profit sectors.

Compliance with ethical standards

Conflict of interest The authors declare that they do not have any conflict of interest.

References

Abdel-Aziz HMM, Hasaneen MNA, Omer AM (2016) Nano chitosan-NPK fertilizer enhances the growth and productivity of wheat plants grown in sandy soil. Span J Agric Res 14:902–911

Alfaro M, Salazar F, Iraira S, Teuber N, Villarroel D, Ramírez L (2008) Nitrogen, phosphorous and potassium losses in a grazing system with different stocking rates in a volcanic soil. Chili J Agric Res 68:146–155

Badawy MEI, Rabea E (2011) A biopolymer chitosan and its derivatives as promising antimicrobial agents against plant pathogens and their applications in crop protection. Int J Carb Chem 2011:29

Barac M, Cabrilo S, Pesic M, Stanojevic S, Zilic S, Macej O (2010) Profile and functional properties of seed proteins from six pea (*Pisum sativum*) genotypes. Intern J Mol Sci 11:4973–4990

Barrenaa R, Casals E, Colóna J, Fonta X, Sáncheza A, Puntesbc V (2009) Evaluation of the ecotoxicity of model nanoparticles. Chemosphere 75:850–857

Baskar V, Venkatesh J, Park SW (2015) Impact of biologically synthesized silver nanoparticles on the growth and physiological responses in *Brassica rapa* ssp. pekinensis. Environ Sci Pollut Res 22:17672–17682

Beenken KE, Smith JK, Skinner RA, Mclaren SG, Bellamy W, Gruenwald MJ, Spencer HJ, Jennings JA, Haggard WO, Smeltzer MS (2014) Chitosan coating to enhance the therapeutic efficacy of calcium sulfate-based antibiotic therapy in the treatment of chronic osteomyelitis. J Biomater Appl 29(4):514–523

Cabaleiro-Lago C, Quinlan-Pluck F, Lynch I, Dawson KA, Linse S (2010) Dual effect of amino modified polystyrene nanoparticles on amyloid β protein fibrillation. ACS Chem Neurosci 1:279–287

Cedervall T, Lynch I, Lindman S, Berggård T, Thulin E, Nilsson H (2007) Understanding the nanoparticle-protein corona using methods to quantify exchange rates and affinities of proteins for nanoparticles. Proc Natl Acad Sci USA 104:2050–2055

Celis R, Adelino MA, Hermosín MC, Cornejo J (2012) Montmorillonite–chitosan bionanocomposites as adsorbents of the herbicide clopyralid in aqueous solution and soil/water suspensions. J Hazard Mater 210:67–76

Corradini E, de Moura MR, Mattoso LHC (2010) A preliminary study of the incorporation of NPK fertilizer into chitosan nanoparticles. Express Polym Lett 4:509–515

da Silva MA, Bode F, Drake AF, Goldoni S, Stevens MM, Dreiss CA (2014) Enzymatically cross-linked gelatin/chitosan hydrogels: tuning gel properties and cellular response. Macromol Biosci 14(6):817–830

DeRosa MC, Monreal C, Schnitzer M, Walsh R, Sultan Y (2010) Nanotechnology in fertilizers. Nat Nanotech 5:91

Di Bucchianico S, Cappellini F, Le Bihanic F, Zhang Y, Dreij K, Karlsson HL (2017) Genotoxicity of TiO2 nanoparticles assessed by mini-gel comet assay and micronucleus scoring with flow cytometry. Mutagen 32:127–137

Dimkpa CO, McLean JE, Martineau N, Britt DW, Haverkamp R, Anderson AJ (2013) Silver nanoparticles disrupt wheat (*Triticum aestivum* L.) growth in a sand matrix. Environ Sci Technol 47:1082–1090

FAO (2015) Food and Agriculture Organization of the United Nations, Rome, Italy. http://faostat.fao.org/default.aspx

Ferraro D, Anselmi-Tamburini U, Tredici IG, Ricci V, Sommi P (2016) Overestimation of nanoparticles-induced DNA damage determined by the comet assay. Nanotoxicol 10:861–870

Gichner T, Patková Z, Száková J, Demnerová K (2006) Toxicity and DNA damage in tobacco and potato plants growing on soil polluted with heavy metals. Ecotox Environ Safe 65:420–426

Gichner T, Žnidar I, Száková J (2008) Evaluation of DNA damage and mutagenicity induced by lead in tobacco plants. Mutat Res Genet Toxicol Environ Mutagen 652:186–190

Good AG, Beatty PH (2011) Fertilizing nature: a tragedy of excess in the commons. PLoS Biol 9(8):e1001124

Gritsch L, Wolfgang CL, Goldmann AH, Boccaccini R (2018) Fabrication and characterization of copper(II)-chitosan complexes as antibiotic-free antibacterial biomaterial. Carbohydr Polym 179:370–378

Hadwiger LA (2013) Multiple effects of chitosan on plant systems: solid science or hype. Plant Sci 208:42–49

Halling-Sorensen B, Jorgensen SE (1993) The removal of nitrogen compound in waste water. Elsevier, Amsterdam

Hasaneen MNA, Abdel-Aziz HMM, El-Bialy DMA, Omer AM (2014) Preparation of chitosan nanoparticles for loading with NPK fertilizer. Afr J Biotech 13:3158–3164

Hossain Z, Mustafa G, Komatsu S (2015) Plant responses to nanoparticle stress. Intern J Mol Sci 16:26644–26653

Iriti M, Faoro F (2008) Abscisic acid mediates the chitosan-induced resistance in plant against viral disease. Plant Physiol Biochem 46:1106–1111

Janes KA, Calvo P, Alonso MJ (2001) Polysaccharide colloidal particles as delivery systems for macromolecules. Adv Drug Deliv Rev 47:83–97

Jiao X, Maimaitiyiming A, Salahou M, Liu K, Guo W (2017) Impact of groundwater level on nitrate nitrogen accumulation in the vadose zone beneath a cotton field. Water 9:171

Joseph T, Morrison M (2006) Nanotechnology in agriculture and food: a nanoforum report, Institute of Nanotechnology May 2006, www.nanoforum.org

Kashyap PL, Xiang X, Heiden P (2015) Chitosan nanoparticle based delivery systems for sustainable agriculture. Int J Biol Macromol 77:36–51

Khalifa NS (2012) Protein expression after NaCl treatment in two tomato cultivars differing in salt tolerance. Acta Biol Crac Bot 54:79–86

Khati P, Chaudhary P, Gangola S, Bhatt P, Sharma A (2017) Nanochitosan supports growth of Zea mays and also maintains soil health following growth. 3 Biotech 7:81

Klosterman SJ, Choi JJ, Hadwiger LA (2003) Analysis of pea HMG-I/Y expression suggests a role in defense gene regulation. Mol Plant Path 4:249–258

Koppen G, Cerda H (1997) Identification of low-dose irradiated seeds using the neutral comet assay. LWT Food Sci Technol 30:452–457

Kumar G, Smith PJ, Payne GF (1999) Enzymatic grafting of a natural product onto chitosan to confer water solubility under basic conditions. Biotechnol Bioeng 63(2):154–165

Kumari M, Mukherjee A, Chandrasekaran N (2009) Genotoxicity of silver nanoparticles in *Allium cepa*. Sci Total Environ 15(19):2456–5243

Kuzma J, Verhage P (2006) Nanotechnology in agriculture and food production: anticipated application, 4th edn. Woodrow Wilson international center for scholars, Washington, DC, pp 1–40

Laemmli UK (1970) Cleavage of structural proteins during the assembly of the head of bacteriophage T4. Nature 227:680–685

Li YZ, Zhao JY, Wu SM, Fan XW, Luo XL, Chen BS (2016) Characters related to higher starch accumulation in cassava storage roots. Sci Rep 6:19823

Lizardi-Mendoza J, Argüelles Monal WM, Goycoolea Valencia FM (2016) Chemical characteristics and functional properties of chitosan. Chitosan in the preservation of agricultural commodities. Elsevier, Amsterdam, pp 3–31

Malerba M, Cerana R (2016) Chitosan effects on plant systems. Inter J Mol Sci 17(7):996

Malerba M, Crosti P, Cerana R (2012) Defense/stress responses activated by chitosan in sycamore cultured cells. Protoplasma 249:89–98

Mondal MMA, Malek MA, Puteh AB, Ismail MR, Ashrafuzzaman M, Naher L (2012) Effect of foliar application of chitosan on growth and yield in okra. Aust J Crop Sci 6:918–921

Morales-Díaz AB, Ortega-Ortiz H, Juarez-Maldonado A, Cadenas-Pliego G, Gonzales-Morales S, Benavides-Mendoza A (2017) Application of nanoelements in plant nutrition and its impact in ecosystems. Adv Nat Sci 8:013001

Nagaonkar D, Shende S, Rai M (2015) Biosynthesis of copper nanoparticles and its effect on actively dividing cells of mitosis in *Allium cepa*. Biotech Prog 31:557–565

Nair PMG, Chung IM (2017) Evaluation of stress effects of copper oxide nanoparticles in *Brassica napus* L. seedlings. 3 Biotech 7:293

Nandhakumar S, Parasuraman S, Shanmugam MM, Rao KR, Chand P, Bhat BV (2011) Evaluation of DNA damage using single-cell gel electrophoresis (Comet Assay). J pharm pharmacother 2:107–111

Niki T, Gladish DK (2001) Changes in growth and structure of pea primary roots (*Pisum sativum* L. cv. Alaska) as a result of sudden flooding. Plant Cell Physiol 42:694–702

Nikolova I, Georgieva M, Stoilov L, Todorova D (2013) Zornica Katerova optimization of neutral comet assay for studying DNA double-strand breaks in pea and wheat. J Bio Sci Biotech 2:151–157

O'Neill A, Sen Gupta B, Phillips DH (2014) Distribution of arsenic and risk assessment of activities on a golf course fertilized with arsenic-containing *Ascophyllum nodosum* seaweed. Sci Total Environ 483:252–259

Osipov A, Arkhangelskaya E, Vinokurov A, Smetanina N, Zhavoronkov A, Klokov D (2014) DNA comet Giemsa staining for conventional bright-field microscopy. Inter J Mol Sci 15:6086–6095

Pang Y, Qin A, Lin X, Yang L, Wang Q, Wang Z et al (2017) Biodegradable and biocompatible high elastic chitosan scaffold is cell-friendly both in vitro and in vivo. Oncotarget 8:35583–35591

Pereira AES, Sandoval-Herrera IE, Zavala-Betancourt SA, Oliveira HC, Ledezma-Pérez AS, Romero J et al (2017) γ-Polyglutamic acid/chitosan nanoparticles for the plant growth regulator gibberellic acid: characterization and evaluation of biological activity. Carbohydr Polym 157:1862–1873

Radhakrishnan Y, Gopal G, Lakshmanan CC, Nandakumar KS (2015) Chitosan nanoparticles for generating novel systems for better applications: a review. J Mol Gene Med S4:005

Rajkishore S (2013) Nanotoxicity at various trophic levels: a review. Biosafety of nanoparticles. Toxicology 8(3):975–982

Ray PC, Yu H, Fu PP (2009) Toxicity and environmental risks of nanomaterials: challenges and future needs. J Environ Sci Health Part C 27:1–35

Roco MC (2011) The long view of nanotechnology development: the National Nanotechnology Initiative at 10 years. J Nanopart Res 13(2):427–445

Rodriguez E, Azevedo R, Fernandes P, Santos C (2011) Cr(VI) induces DNA damage, cell cycle arrest and polyploidization: a flow cytometric and comet assay study in *Pisum sativum*. Chem Res Toxicol 24:1040–1047

Schneider CA, Rasband WS, Eliceiri KW (2012) NIH Image to ImageJ: 25 years of image analysis. Nat Methods 9(7):671

Scott N, Chen H (2013) Nanoscale science and engineering for agriculture and food systems. Ind Biotech 9:17–18

Sedbrook JC, Chen R, Masson PH (1999) ARG1 (altered response to gravity) encodes a DnaJ-like protein that potentially interacts with the cytoskeleton. Proc Natl Acad Sci USA 96:1140–1145

Siddiqi KS, Husen A (2016) Engineered gold nanoparticles and plant adaptation potential. Nanoscale Res Lett 11:400

Sivamani E, DeLong RK, Qu R (2009) Protamine-mediated DNA coating remarkably improves bombardment transformation efficiency in plant cells. Plant Cell Rep 28:213–221

Vold IMN, Varum KM, Guibal E, Smidsrød O (2003) Binding of ions to chitosan—selectivity studies. Carbohydr Polym 54:471–477

Wang L, Hua D, He J, Duan Y, Chen Z, Hong X et al (2011) Auxin Response Factor2 (ARF2) and its regulated homeodomain gene HB33 mediate abscisic acid response in arabidopsis. PLoS Gen 7:e1002172

Wang Y, Xu C, Du LQ, Cao J, Liu JX, Su X et al (2013) Evaluation of the comet assay for assessing the dose-response relationship of DNA damage induced by ionizing radiation. Int J Mol Sci 14:22449–22461

White PJ, Brown PH (2010) Plant nutrition for sustainable development and global health. Ann Bot 105:1073–1080

Yan XL, Dai TF, Jia LM (2018) Evaluation of the cumulative effect of drip irrigation and fertigation on productivity in a poplar plantation. Ann For Sci 75:5

Yazdani MR, Virolainen E, Conley K, Vahala R (2018) Chitosan–Zinc(II) complexes as a bio-sorbent for the adsorptive abatement of phosphate: mechanism of complexation and assessment of adsorption performance. Polym 10(1):25

Yin H, Zhao X, Bai X, Du Y (2010) Molecular cloning and characterization of a *Brassica napus* L. MAP kinase involved in oligochitosan-induced defense signaling. Plant Mol Biol Rep 28:292–301

Zaman M, Ahmad E, Qadeer A, Rabbani G, Khan RH (2014) Nanoparticles in relation to peptide and protein aggregation. Int J Nanomed 9:899–912

Zawaski C, Ma C, Strauss SH, French D, Meilan R, Busov VB (2012) PHOTOPERIOD RESPONSE 1 (PHOR1)-like genes regulate

shoot/root growth, starch accumulation, and wood formation in Populus. J Exp Bot 63:5623–5634
Zhang Y (2003) Transcriptional regulation by histone ubiquitination and deubiquitination. Genes Dev 17:2733–2740
Zivic F, Grujovic N, Mitrovic S, Ahad IU, Brabazon D (2018) Characteristics and applications of silver nanoparticles. Commercialization of nanotechnologies—a case study approach. Springer, New York, pp 227–273
Zuppini A, Baldan B, Millioni R, Favaron F, Navazio L, Mariani P (2003) Chitosan induces Ca^{2+}-mediated programmed cell death in soybean cells. New phytol 161(2):557–568